

What drives chorus wave frequency chirping? F SCI

Cite as: Phys. Plasmas **32**, 100703 (2025); doi: 10.1063/5.0289277

Submitted: 7 July 2025 · Accepted: 18 September 2025 ·

Published Online: 10 October 2025



View Online



Export Citation



CrossMark

Xin Tao,^{1,a)} Fulvio Zonca,² and Liu Chen³

AFFILIATIONS

¹Department of Geophysics and Planetary Sciences, University of Science and Technology of China, Hefei, China

²Center for Nonlinear Plasma Science and C.R. ENEA Frascati, C.P. 65, 00044 Frascati, Italy

³Department of Physics and Astronomy, University of California, Irvine, California 92697, USA

^{a)}Author to whom correspondence should be addressed: xtao@ustc.edu.cn

ABSTRACT

For over 50 years, chorus wave frequency chirping has been regarded as a nonlinear phenomenon driven by the hot electron current density aligned with the wave magnetic field (δj_B). However, recent theoretical models have challenged the crucial role played by δj_B . Here, using modified first-principles particle simulations, we demonstrate that chirping can occur even in the absence of δj_B . This result not only clarifies the physical mechanism governing chorus wave evolution but also has broader implications for nonlinear frequency chirping in other wave modes and plasma environments.

© 2025 Author(s). All article content, except where otherwise noted, is licensed under a Creative Commons Attribution-NonCommercial-NoDerivs 4.0 International (CC BY-NC-ND) license (<https://creativecommons.org/licenses/by-nc-nd/4.0/>). <https://doi.org/10.1063/5.0289277>

Nonlinear frequency chirping, characterized by rapid temporal variations in wave frequency, is a ubiquitous phenomenon observed in diverse plasma environments.^{1–8} A prominent example is whistler-mode chorus waves in planetary magnetospheres,^{6,9} which exhibit quasi-coherent, narrowband emissions with dynamically changing frequencies. When rendered audibly, these emissions sound like birds chirping at dawn, hence their name. Figure 1 illustrates a representative chorus wave spectrum captured by THEMIS A.¹⁰ Similar behavior is observed in electromagnetic ion cyclotron waves in space plasmas^{4,7} and Alfvén waves in fusion devices.^{3,11} This phenomenon is of fundamental interest as it underpins the generation of coherent emissions in plasmas and drives rapid, nonlinear transport of energetic particles—processes critical to space weather¹² and fusion plasma confinement.^{13,14} Studies on wave-particle interactions in other plasma regimes have also been reported.^{15–18} Despite decades of research and broad consensus on the role of nonlinear wave-particle interactions, the precise mechanisms governing frequency chirping remain a subject of active debate.^{19–28}

One approach to understanding the frequency chirping is to make use of the narrowband nature of chorus waves from the beginning.^{20,24} As shown in Fig. 1, the instantaneous bandwidth of chorus is only about 200 Hz. Assuming a narrowband parallel propagating plasma wave and applying Maxwell equations, Omura and Nunn²⁴ arrived at the following two equations:

$$\left(\frac{\partial}{\partial t} + v_g \frac{\partial}{\partial z}\right) \delta B = -\frac{\mu_0 v_g}{2} \delta j_E, \quad (1)$$

$$\left[\frac{c^2 k^2}{\omega^2} - 1 - \frac{\omega_{pe}^2}{\omega(\Omega_e - \omega)}\right] \delta B = \frac{\mu_0 c^2 k}{\omega^2} \delta j_B, \quad (2)$$

where v_g is the wave group velocity, z is the coordinate along the field line, c is the speed of light, ω is the wave frequency, k is the wave number, Ω_e is the unsigned electron cyclotron frequency, and δB is the wave magnetic field strength. These equations are derived under the assumption of a two-component electron plasma, consisting of a cold background component and a hot, energetic component. In this context, δj_E represents the component of the hot electron current, δj_h , parallel to the wave electric field, while δj_B is the component parallel to the wave magnetic field. It is straightforward to see that δj_E affects wave amplitude, while δj_B directly affects the wave frequency, leading to a frequency shift. Models using δj_B to explain the frequency chirping of chorus has a long history.^{20,24} For example, the “sequential triggering model” proposed by Omura *et al.*²⁴ is a recent and well-known example. In this model, a triggering wave with an initial frequency ω_0 drives nonlinear electron dynamics, generating a nonlinear current. The δj_B component of this current leads to a frequency shift $\delta\omega$, resulting in a new wave at $\omega + \delta\omega$. The newly formed wave can then act as a triggering wave, initiating further frequency shifts in the same direction. Repeated cycles of this process produce a continuous upward frequency drift, ultimately generating the characteristic chirping structure. In the following discussion, we refer to this mechanism as the “single-wave” approach, as it builds on the

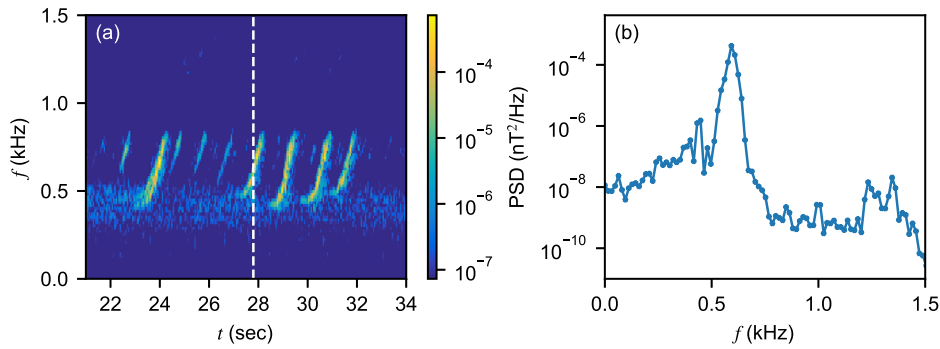


FIG. 1. Chorus waves from satellite observations. (a) Spectrogram of magnetic field fluctuations showing chorus emissions observed by THEMIS A on July 26, 2008. The x -axis coordinate is the seconds since 13:26:00 UTC. Color-coded is the power spectral density of wave magnetic field. The emissions exhibit discrete rising-tone elements with an instantaneous bandwidth of about 200 Hz. (b) Corresponding power spectral density at the time indicated by the vertical white dashed line in the left panel, highlighting the narrowband nature of the observed waves.

narrowband nature of the wave from the beginning. The single-wave approach fundamentally relies on δj_B to explain frequency chirping.

A different approach to understanding frequency chirping explicitly utilizes the continuous wave spectrum supported by the background plasma. We refer to this as the “multi-wave” approach, in which frequency chirping is explained as the selective amplification of narrowband emissions from a broadband spectrum of background wave modes. This chirping process corresponds to the maximization of wave-particle power transfer.²⁹ For example, in the recently proposed “Trap-Release-Amplify” (TaRA) model²⁶ of chorus waves, the excited narrowband waves are those among the broadband background modes that can resonate with nonlinearly formed electron phase space structures. Correspondingly, the process naturally maximizes wave-particle power transfer. The narrowband nature of the excited waves arises from the localization of the nonlinear structures in phase space, a consequence of coherent wave-particle interactions. In the nonlinear wave-particle interaction stage, the maximization of power transfer is explicitly described within the framework by Zonca *et al.*²⁸ The frequency drift corresponds to the propagation of the maximum growth rate in frequency space. In this multi-wave approach, the δj_B component of the resonant current does not play a critical role in explaining the occurrence of nonlinear frequency chirping.^{26–28} Provided that the cold plasma dominates, the excited narrowband waves satisfy the dispersion relation determined by the cold plasma. Animations illustrating the differences between the single-wave and multi-wave approaches are included in the [supplementary material](#).

Other models, inspired by devices such as the backward wave oscillator (BWO)^{21,23,30,31} and the free-electron laser (FEL),³² have also been proposed. The BWO model requires a step-like electron distribution that could arise from linear instability,²¹ while the FEL model mainly addresses wave amplification and does not directly treat frequency chirping.

Both the single-wave and multi-wave approaches have been supported by different reduced numerical models. The Vlasov Hybrid Simulation model,³³ which adopts the single-wave perspective, modifies the wave frequency via the electron current parallel to the wave magnetic field (δj_B). In contrast, Zonca *et al.*²⁸ derived and solved governing equations of chorus wave frequency chirping based on a multi-wave theoretical framework, demonstrating frequency chirping without invoking δj_B . However, reduced models inherently incorporate the specific physical assumptions on which they are based, limiting their

ability to serve as definitive tests for distinguishing between these approaches. This makes a first-principles approach essential for directly assessing the role of δj_B in chorus wave dynamics.

In this study, we present first-principles particle-in-cell (PIC) simulations that do not embed any specific assumptions about the chirping mechanism and demonstrate that nonlinear frequency chirping can occur in the absence of δj_B , thereby providing direct support for the multi-wave approach. PIC simulations of chorus wave frequency chirping were first demonstrated by Katoh *et al.*³⁴ in 2007. In this work, we use the PIC code DAWN^{35,36} to simulate chorus waves. In the standard setup for PIC simulations of parallel-propagating chorus waves, the Ampère–Maxwell’s law to be solved is

$$\frac{\partial}{\partial t} \delta \mathbf{E} = c^2 \nabla \times \delta \mathbf{B} - \frac{1}{\epsilon_0} (\delta \mathbf{j}_c + \delta \mathbf{j}_h), \quad (3)$$

where $\delta \mathbf{j}_c$ is the current density due to cold electrons, and $\delta \mathbf{j}_h$ is the current density due to hot electrons. The background magnetic field, \mathbf{B}_0 , is primarily aligned with the z -axis and varies in strength according to $B_z = B_{0z}(1 + \zeta z^2)$, where the parameter ζ characterizes the degree of field inhomogeneity. This form approximates the variation in the strength of the dipole magnetic field along a field line near the equator, where chorus waves are typically generated. In this configuration, the waves are assumed to propagate parallel to the background field, meaning they travel along the z direction. As a result, the wave electric ($\delta \mathbf{E}$) and magnetic ($\delta \mathbf{B}$) fields have only x and y components. The hot electron distribution is modeled as bi-Maxwellian, with a temperature (T) anisotropy such that $T_{\perp} > T_{\parallel}$, where “ \perp ” and “ \parallel ” refer to directions perpendicular and parallel to the background magnetic field, respectively.

To explicitly test whether δj_B drives frequency chirping, we modify the current deposition step in the simulation: after depositing the hot electron current densities onto the simulation grid at each time step, we remove the δj_B component by replacing

$$\delta \mathbf{j}_h \rightarrow \delta \mathbf{j}_h - \left(\delta \mathbf{j}_h \cdot \delta \hat{\mathbf{B}} \right) \delta \hat{\mathbf{B}} \quad (4)$$

before updating Eq. (3). Here, $\delta \hat{\mathbf{B}}$ is the unit vector in the direction of the wave magnetic field. This operation effectively isolates only the δj_E component in the Maxwell equations. Under this modified setup, if we apply the same narrowband wave assumption, the resulting system reduces to Eqs. (1) and (2) without δj_B , allowing a direct test of its role in nonlinear frequency chirping.

For the present study, we simulate the same chorus wave event as in Tao *et al.*,^{26,36} but with the δj_B component removed. The background magnetic field inhomogeneity parameter is $\xi = 2.155 \times 10^{-5} d_e^{-2}$, with $d_e \equiv c/\Omega_{e0}$, and the hot electron density is 6% of the total electron number density. Here c is the speed of light in vacuum, and Ω_{e0} is the electron cyclotron frequency at $z = 0$. The spatial and temporal grid resolutions are $dz = 0.05 d_e$ and $dt = 0.02 \Omega_{e0}^{-1}$, respectively. The ratio of plasma frequency to electron gyrofrequency is $\omega_{pe}/\Omega_{e0} = 5.0$. The simulation domain contains 6554 cells, spanning $z = -163 d_e$ to $163 d_e$, with 4000 particles per cell to reduce statistical noise. To excite discrete chorus elements, we vary the temperature anisotropy across a series of runs. The final perpendicular and parallel thermal velocities (w) are $w_{\perp} = 0.47c$ and $w_{\parallel} = 0.2c$.

The simulation results are presented in Fig. 2. The left panel shows a sample of the unit vectors of the hot electron current density, $\delta \hat{j}_h$, and wave magnetic field, $\delta \hat{B}$, at a specific time, $t\Omega_{e0} = 2300$, and location, $z/d_e = 30$. As intended, the current density is clearly perpendicular to the wave magnetic field, confirming the successful removal of the δj_B component. In fact, all recorded hot electron current densities throughout the simulation are perpendicular to the wave magnetic field, as designed.

The right panel of Fig. 2 shows the spectrogram of the wave magnetic field power spectral density at the same location, $z/d_e = 30$. Despite some background noise, three distinct chorus elements with frequency chirping can be clearly identified. These elements exhibit similar chirping rates of approximately $\partial\omega/\partial t \approx 1.7 \times 10^{-4} \Omega_{e0}^{-2}$, comparable to the rate ($2.6 \times 10^{-4} \Omega_{e0}^{-2}$) observed in previous standard simulations²⁶ of chorus with $\delta j_B \neq 0$. Unlike the earlier results, which showed only one element, the present simulation produces three. This difference is likely due to the higher temperature anisotropy used here.

These results demonstrate that frequency chirping can occur without δj_B , providing strong support for the multi-wave approach as a possible explanation for this phenomenon. Although the present simulation focuses on whistler-mode chorus waves in space plasmas, its implications extend to other wave modes that exhibit frequency chirping. In space plasmas, a notable example is the frequency chirping of electromagnetic ion cyclotron waves.⁷ In fusion plasmas, chirping is observed in Alfvénic modes such as fishbone and energetic particle modes.³⁷ A general theoretical framework unifying these diverse chirping phenomena based on the multi-wave approach is under development and will be published elsewhere. For chorus waves specifically, such a theoretical framework is provided by Zonca *et al.*,²⁸ where the

evolution of the electron phase space distribution is governed by a Dyson-type equation.

It is useful to clarify the distinction between the frequency shift $\delta\omega$ caused by δj_B and the phenomenon of frequency chirping. As shown in Eq. (2), δj_B produces a shift in wave frequency. Notably, Eqs. (1) and (2) are valid in both linear and nonlinear regimes. In the case of chorus waves, the current density is generated by the nonlinear motion of electrons. However, a nonlinear frequency shift is not equivalent to frequency chirping. In the sequential triggering model,²⁴ chirping is explained as a sequence of frequency shifts. This model assumes that all frequency shifts occur in the same direction, matching the direction of the overall chirping. In contrast, Zonca *et al.*²⁸ performed a self-consistent calculation of the frequency shift, fully accounting for particle dynamics. Their results show that the frequency shift oscillates in time and does not maintain a consistent sign aligned with the overall frequency chirping. This distinction highlights that while δj_B may contribute to wave amplitude and other related quantities, it is not essential for producing frequency chirping itself.

We also comment briefly on the challenge of distinguishing between these models using satellite observations or laboratory plasma experiments. In space or laboratory, one cannot simply “turn off” δj_B , as we do in our numerical experiment. The δj_B may be present due to the consistency requirement of Maxwell equations; however, its presence does not imply causality. That is, δj_B may appear as a consequence of wave evolution, rather than as its driver. A possible observational approach would be to compare wave events with and without frequency chirping and examine the correlation between the presence of δj_B and wave frequency chirping. Although such studies would not involve direct control experiments, they could provide statistical evidence on whether δj_B is essential for frequency chirping.

Finally, we point out that single-wave models may be relevant to systems where only one mode, or a narrowband set of modes, is supported at a given time, whereas multi-wave models apply when the system supports a broadband, continuous spectrum of waves. This is the fundamental reason why chorus chirping has a one-on-one correspondence with energetic particle mode chirping in fusion plasmas.^{27,28}

In summary, our modified PIC simulation provides the first direct, first-principles numerical demonstration that nonlinear frequency chirping of chorus waves can occur without δj_B . By removing δj_B from the simulation, we show unambiguously that this component is not the driver of frequency chirping. Due to the simplicity and clarity of the setup, the numerical experiment is robust and easily reproducible. These results offer compelling support for the multi-wave

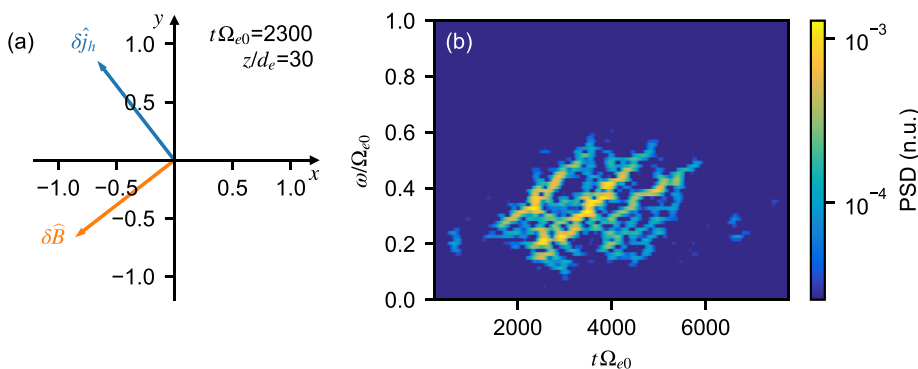


FIG. 2. Results of a modified PIC simulation. (a) Unit vectors of hot electron current density, $\delta \hat{j}_h$, and wave magnetic field, $\delta \hat{B}$, at $t\Omega_{e0} = 2300$ and $z/d_e = 30$, showing $\delta \hat{j}_h \perp \delta \hat{B}$ as intended. (b) Spectrogram of wave magnetic field at the same location in normalized units (n.u.), showing three upward-chirping chorus elements.

approach and challenge the long-standing assumption that δj_B is the underlying cause of chorus frequency chirping.

See the [supplementary material](#) for animations of single and multiple pendulums that demonstrate frequency chirping in the single-wave and multi-wave models, respectively.

This work was supported by the Strategic Priority Research Program of the Chinese Academy of Sciences (Grant No. XDB0560000) and the National Natural Science Foundation of China (Grant No. 42174182).

AUTHOR DECLARATIONS

Conflict of Interest

The authors have no conflicts to disclose.

Author Contributions

Xin Tao: Conceptualization (equal); Formal analysis (equal); Funding acquisition (equal); Investigation (equal); Methodology (equal); Project administration (equal); Software (equal); Validation (equal); Visualization (equal); Writing – original draft (equal). **Fulvio Zonca:** Conceptualization (equal); Investigation (equal); Methodology (equal); Visualization (equal); Writing – review & editing (equal). **Liu Chen:** Conceptualization (equal); Investigation (equal); Methodology (equal); Writing – review & editing (equal).

DATA AVAILABILITY

The data that support the findings of this study are available from the corresponding author upon reasonable request.

REFERENCES

- ¹B. T. Tsurutani and E. J. Smith, *J. Geophys. Res.* **79**, 118, <https://doi.org/10.1029/JA079i001p00118> (1974).
- ²W. J. Burtis and R. A. Helliwell, *J. Geophys. Res.* **80**, 3265, <https://doi.org/10.1029/JA080i022p03265> (1975).
- ³K. McGuire, R. Goldston, M. Bell, M. Bitter, K. Bol, K. Brau, D. Buchenauer, T. Crowley, S. Davis, F. Dylla, H. Eubank, H. Fishman, R. Fonck, B. Grek, R. Grimm, R. Hawryluk, H. Hsuan, R. Hulse, R. Izzo, R. Kaita, S. Kaye, H. Kugel, D. Johnson, J. Manickam, D. Manos, D. Mansfield, E. Mazzucato, R. McCann, D. McCune, D. Monticello, R. Motley, D. Mueller, K. Oasa, M. Okabayashi, K. Owens, W. Park, M. Reusch, N. Sauthoff, G. Schmidt, S. Sesnic, J. Strachan, C. Surko, R. Slusher, H. Takahashi, F. Tenney, P. Thomas, H. Towner, J. Valley, and R. White, *Phys. Rev. Lett.* **50**, 891 (1983).
- ⁴J. S. Pickett, B. Grison, Y. Omura, M. J. Engebretson, I. Dandouras, A. Masson, M. L. Adrian, O. Santolík, P. M. E. Décreau, N. Cornilleau-Wehrin, and D. Constantinescu, *Geophys. Res. Lett.* **37**, L09104, <https://doi.org/10.1029/2010GL042648> (2010).
- ⁵W. Sawaguchi, Y. Harada, and S. Kurita, *Geophys. Res. Lett.* **48**, e2020GL091100, <https://doi.org/10.1029/2020GL091100> (2021).
- ⁶S. Teng, Y. Wu, Y. Harada, J. Bortnik, F. Zonca, L. Chen, and X. Tao, *Nat. Commun.* **14**, 3142 (2023).
- ⁷Z. An, X. Tao, F. Zonca, and L. Chen, *Geophys. Res. Lett.* **51**, e2023GL106456, <https://doi.org/10.1029/2023GL106456> (2024).
- ⁸W. D. Fu, H. S. Fu, Y. F. Wu, X. Tao, Y. Yu, W. Z. Zhang, and J. B. Cao, *Geophys. Res. Lett.* **52**, e2024GL112859, <https://doi.org/10.1029/2024GL112859> (2025).
- ⁹G. B. Hospodarsky, T. F. Averkamp, W. S. Kurth, D. A. Gurnett, J. D. Menietti, O. Santolík, and M. K. Dougherty, *J. Geophys. Res.* **113**, A12206, <https://doi.org/10.1029/2008JA013237> (2008).
- ¹⁰V. Angelopoulos, *Space Sci. Rev.* **141**, 5 (2008).
- ¹¹W. W. Heidbrink, *Phys. Plasmas* **15**, 055501 (2008).
- ¹²A. V. Artemyev, A. A. Vasiliev, D. Mourenas, O. V. Agapitov, V. Krasnoselskikh, D. Boscher, and G. Rolland, *Geophys. Res. Lett.* **41**, 5727, <https://doi.org/10.1002/2014GL061380> (2014).
- ¹³R. B. White, R. J. Goldston, K. McGuire, A. H. Boozer, D. A. Monticello, and W. Park, *Phys. Fluids* **26**, 2958 (1983).
- ¹⁴F. Zonca, L. Chen, S. Briguglio, G. Fogaccia, A. V. Milovanov, Z. Qiu, G. Vlad, and X. Wang, *Plasma Phys. Controlled Fusion* **57**, 014024 (2015).
- ¹⁵K. Arshad and S. Poedts, *Phys. Plasmas* **27**, 122904 (2020).
- ¹⁶K. Arshad, M. Lazar, S. Mahmood, A. ur Rehman, and S. Poedts, *Phys. Plasmas* **24**, 033701 (2017).
- ¹⁷K. Arshad, S. Poedts, and A. Dahshan, *AIP Adv.* **12**, 105319 (2022).
- ¹⁸K. Arshad, Y. G. Maneva, and S. Poedts, *Phys. Plasmas* **24**, 093708 (2017).
- ¹⁹R. A. Helliwell, *J. Geophys. Res.* **72**, 4773, <https://doi.org/10.1029/JZ072i019p04773> (1967).
- ²⁰D. Nunn, *Planet. Space Sci.* **22**, 349 (1974).
- ²¹V. Y. Trakhtengerts, *J. Geophys. Res.* **100**, 17205, <https://doi.org/10.1029/95JA00843> (1995).
- ²²V. Y. Trakhtengerts, A. G. Demekhov, E. E. Titova, B. V. Kozelov, O. Santolík, D. Gurnett, and M. Parrot, *Phys. Plasmas* **11**, 1345 (2004).
- ²³A. G. Demekhov and V. Y. Trakhtengerts, *Radiophys. Quantum Electron.* **51**, 880 (2008).
- ²⁴Y. Omura and D. Nunn, *J. Geophys. Res.* **116**, A05205, <https://doi.org/10.1029/2010JA016280> (2011).
- ²⁵X. Tao, F. Zonca, and L. Chen, *Geophys. Res. Lett.* **44**, 3441–2017GL072624, <https://doi.org/10.1002/2017GL072624> (2017).
- ²⁶X. Tao, F. Zonca, and L. Chen, *J. Geophys. Res. Space Phys.* **126**, e2021JA029585, <https://doi.org/10.1029/2021JA029585> (2021).
- ²⁷F. Zonca, X. Tao, and L. Chen, *Rev. Mod. Plasma Phys.* **5**(1), 8 (2021).
- ²⁸F. Zonca, X. Tao, and L. Chen, *J. Geophys. Res. Space Phys.* **127**, e2021JA029760, <https://doi.org/10.1029/2021JA029760> (2022).
- ²⁹L. Chen and F. Zonca, *Rev. Mod. Phys.* **88**, 015008 (2016).
- ³⁰V. Y. Trakhtengerts, A. G. Demekhov, E. E. Titova, B. V. Kozelov, O. Santolík, E. Macusova, D. Gurnett, J. S. Pickett, M. J. Rycroft, and D. Nunn, *Geophys. Res. Lett.* **34**, L02104, <https://doi.org/10.1029/2006GL027953> (2007).
- ³¹A. G. Demekhov, U. Taubenschuss, and O. Santolík, *J. Geophys. Res. Space Phys.* **122**, 166, <https://doi.org/10.1002/2016JA023057> (2017).
- ³²B. Bonham and A. Bhattacharjee, “Whistler chorus amplification in the magnetosphere: A nonlinear free-electron laser model based on the Ginzburg-Landau equation,” [arXiv:2506.06167](https://arxiv.org/abs/2506.06167) (2025).
- ³³D. Nunn, *Comput. Phys. Commun.* **60**(1), 1 (1990).
- ³⁴Y. Katoh and Y. Omura, *Geophys. Res. Lett.* **34**, L03102 (2007).
- ³⁵X. Tao, *J. Geophys. Res. Space Phys.* **119**, 3362, <https://doi.org/10.1002/2014JA019820> (2014).
- ³⁶X. Tao, F. Zonca, and L. Chen, *Plasma Phys. Controlled Fusion* **59**, 094001 (2017).
- ³⁷L. Chen, R. B. White, and M. N. Rosenbluth, *Phys. Rev. Lett.* **52**, 1122 (1984).